

Optical and thermal stability in $\text{Ge}_x\text{Se}_{10}\text{Te}_{90-x}$ chalcogenide films

Y. G. WANG¹, M. L. FANG², R. M. WANG³, L. S. YANG³, J. Y. LIU³, J. S. DING³, Y. PAN⁴, X. Q. SU^{3,*}

¹*School of Mechanics and Photoelectric Physics, Anhui University of Science and Technology, Huainan, 232001, China*

²*School of Mathematics and Big Data, Anhui University of Science and Technology, Huainan, 232001, China*

³*School of Physics and Optoelectronic Engineering, Beijing University of Technology, Beijing 100124, China*

⁴*College of Science, Xi'an University of Architecture and Technology, Xi'an, 710055, China*

$\text{Ge}_x\text{Se}_{10}\text{Te}_{90-x}$ chalcogenide thin films with varied Ge content from $x=17.5$ to 27.5 were deposited by e-beam evaporation and their optical properties were investigated under various thermal annealing conditions. The results show that $\text{Ge}_{22.5}\text{Se}_{10}\text{Te}_{67.5}$ film has a minimal change against thermal annealing in optical band gap, refractive index and thickness, and thus is the most stable composition for the applications in chalcogenide-based optical devices.

(Received January 14, 2025; accepted December 4, 2025)

Keywords: Chalcogenide, Thin film, Thermal annealing, Stability

1. Introduction

Chalcogenide glasses have excellent transmission from the visible to the far infrared, high linear and nonlinear refractive index, low phonon energy, making them suitable for applications in various area including night vision, infrared optics, phase change memory, and so on [1-3]. Se-based glasses usually have a transmission edge up to $15\text{ }\mu\text{m}$. By incorporating Te into Se-based glasses, the transmission edge can shift further into the far infrared region, reaching up to $25\text{ }\mu\text{m}$ [4]. Additionally, the third-order nonlinearity in Te-based glasses is also significantly enhanced due to more metallic nature and heavier atomic mass of Te [5,6]. Moreover, Selenium based glasses usually have a large glass-forming region, which facilitate their preparation. In contrast, Te-based glasses are prone to crystallization, necessitating rapid quenching to produce homogeneous materials. Such properties render Te-based glasses highly useful in phase change memory applications [7,8].

In this study, we concentrate on the properties of the Ge-Se-Te thin films, motivated by the potential applications to combine the advantages of both Se- and Te-based glasses. For example, broad transmission and high optical nonlinearity can be obtained in Ge-Se-Te compared with that in pure Ge-Se glasses, and the crystallization rate can be tuned in Ge-Se-Te for the application in phase change memory. Especially, chalcogenide glasses in the form of high-quality thin film have many important applications in practical devices like optical waveguide [1,2], phase change memory [7,8] and absorbers in thin film solar cells [9]. Ge-Se-Te films have been studied extensively, for instance, Cernosek et al. reported the glass transition and crystallization temperatures decrease with increasing Te due to increasing $\text{GeTe}_{2/2}$ instead of $\text{GeSe}_{4/2}$ structural units. The refractive index of thin films increases with higher tellurium content, while the optical band gap of the thin

films decreases with increasing Te content [6]. Sati et al. investigated the nonlinear optical properties of $\text{Ge}_{10}\text{Se}_{90-x}\text{Te}_x$ ($x = 0, 10, 20, 30, 40, 50$) thin films as a function of composition and substrate deposition temperatures (303, 363, and 423 K), and found that, nonlinearity increases with increasing Te content and also with increasing substrate temperature [10]. Noda et al. investigated structural changes of amorphous Ge, GeSe_2 and GeSeTe films by illumination and annealing, and found the existence of photo-induced instability in GeSeTe film [11]. Tomelleri et al. investigated the electrical, optical and structural properties of $\text{GeSe}_{1-x}\text{Te}_x$ thin films with $0.16 < x < 1$ prepared by co-sputtering of GeSe and GeTe target, and demonstrated that Se-rich GeSeTe thin films promising for the applications in memory devices [7]. The nonlinear optical properties of $\text{Ge}_{10}\text{Se}_{90-x}\text{Te}_x$ ($x = 0, 10, 20, 30, 40, 50$) thin films have been investigated as functions of compositions and substrate deposition temperatures (303, 363, and 423 K). The third-order nonlinear susceptibility and nonlinear refractive index have been estimated. Nonlinear refractive index increases with Te content and also with increasing substrate temperature. Among the investigated compositions of $\text{Ge}_{10}\text{Se}_{90-x}\text{Te}_x$, the $\text{Ge}_{10}\text{Se}_{40}\text{Te}_{50}$ composition shows more prominent nonlinear refractive index in comparison with pure silica.

However, the films prepared at vacuum typically contain more defects than their bulk counterpart. While the film-based devices are exposed to high energy laser or pulsed current in optical and electrical applications, the performance of the films-based devices would be deteriorated by the existence of these defects, leading to decayed lifetimes of the devices [12-14]. Therefore, it is crucial to develop high-quality GeSeTe film with stable structural and optical properties. Despite this, the impact of

different annealing times on the optical properties of GeSeTe thin films has seldomly been studied yet.

In this paper, $\text{Ge}_x\text{Se}_{10}\text{Te}_{90-x}$ bulk glasses and thin films were prepared, and thermal stability of the films was investigated under different annealing temperature and time. We fixed Se content at 10% in order to compare the monotonous change of the physical properties as a function of Ge content. The results showed that, while most of the annealing films have changes in the optical parameters, $\text{Ge}_{22.5}\text{Se}_{10}\text{Te}_{67.5}$ composition remains relatively stable against thermal annealing. Therefore, it is considered the best material for the fabrication of Te-based optical and electrical devices.

2. Experiments

$\text{Ge}_x\text{Se}_{10}\text{Te}_{90-x}$ glasses (with $x=17.5, 20, 22.5, 25$ and 27.5) were prepared by the melt-quenching method. High purity (5N) Ge, Se, Te raw materials were weighted and placed into a silica tube. After evacuating the tube to 10^{-3}Pa , it was sealed and put into a rocking furnace. Then, the temperature was raised to $900\text{ }^\circ\text{C}$ and the mixtures were further homogenized for 12 h. The silica tube containing the mixtures were quenched in water and then the glasses were taken out and cut into glass tablets.

The films were deposited by e-beam evaporation with three independent evaporation boats for Ge, Se and Te on thermal oxidation silicon and quartz wafers. Prior to the experiments, the substrates were ultrasonically cleaned by deionized water and ethanol solution. The base pressure was evacuated to $3.1\times 10^{-5}\text{ Pa}$, and a current of 50-80 mA, 10-15 mA, and 3-5 mA was passed through, respectively, a tungsten filament to three evaporation source. The thickness of the film was in-situ monitored by the quartz oscillator installed in the chamber. Energy dispersive x-ray

spectrometer (EDX) was employed to examine the composition of the film over several different positions on the surface.

The glass transition temperature T_g was measured using a differential scanning calorimeter (Shimadzu DSC-50) with 10K/min scanning rate in a nitrogen gas flow of 30mL/min. The density of the glasses was measured using a Mettler H₂O balance (Mettler-Toledo Ltd., Switzerland) with a MgO crystal used as a reference. The as-deposited films were vacuum-annealed at a temperature that was $20\text{ }^\circ\text{C}$ below its respective T_g for different times. X-ray diffraction (XRD) with a scanning angle 2θ range from 10° to 60° was used to probe the possible crystallization. The transmission and absorption spectra of the films were measured at a range from 400 to 2500 nm. The films thickness and refractive index were further measured by infrared variable angle spectroscopic ellipsometry (IR-VASE).

3. Results and discussion

We measured the glass transition temperature T_g and the density of the glasses. Fig.1 shows the results where T_g increases and the density decreases with increasing Ge content. It is well known that Ge is four-coordinated, while both Se and Te are typically two-coordinated in most cases in chalcogenide glasses [2,3]. Therefore, with increasing Ge contents, more crosslinks of the glass network will be formed, leading to an increase in T_g . On the other hand, the replacement of Te with Ge results in decreasing density since atomic mass of Ge is less than that of Te.

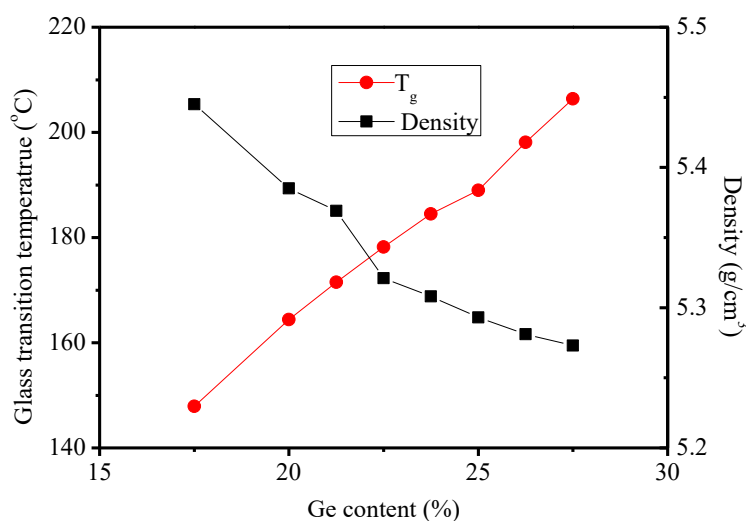


Fig. 1. Glass transition temperature T_g and density as a function of Ge content in the glasses (colour online)

X-ray diffraction measurements indicated that all the films were amorphous. The film compositions were examined using an energy dispersive x-ray spectrometer

and the difference between the film and the corresponding bulk glass is less than 1%. Therefore, the $\text{Ge}_x\text{Se}_{10}\text{Te}_{90-x}$ films with similar compositions as their bulk counterparts

were marked as Ge 17.5, Ge20, Ge22.5, Ge25 and Ge27.5, respectively, and selected for the characterization of their optical properties in the rest art of the paper.

Fig. 2 shows the refractive indices of the films at different wavelengths measured by infrared variable angle spectroscopic ellipsometry. The refractive index decreases with increasing wavelength for each film. For example, Ge

17.5 film has a refractive index at 3.47 at 2 μm but this decreases to 3.31 at 14 μm . On the other hand, for the certain wavelength, the refractive index decreases with increasing Ge content in the film.

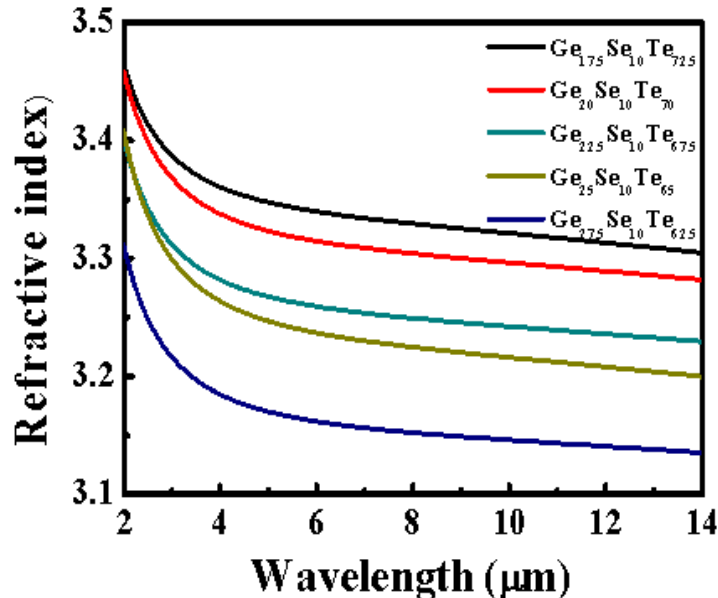


Fig. 2. Refractive indices of the films at different wavelengths (colour online)

Fig. 3(a) presents the change of the refractive index at 5 μm with increasing Ge content in the films. The reason why we compare the refractive index at 5 μm is two folded: one is that Te-based glasses usually are used for longer wavelength, another is that the infrared variable angle spectroscopic ellipsometry is working at a wavelength range from 1.7 to 25 μm , and thus 5 μm is far away from its low detecting limit to avoid any uncertainty. According to the well-established Lorentz–Lorenz relationship [15,16], the refractive index is related to the density and the polarizability. Here we have no data related to the density of each film. Knotek et al. investigated the difference of the density in As-S and As-Se chalcogenide bulk glasses and thin films, being less than 5 % [17]. Since each film in the paper has similar composition as its bulk counterpart, we consider the film density is approximately same as the bulk density. As shown in Fig.1, the density decreases with increasing Ge content. Since Te and Ge have similar electronic polarizability, the change in the density is

believed to account for the change of the refractive index observed in Fig. 3(a).

The as-prepared films were annealed at a temperature which is 20 $^{\circ}\text{C}$ less than their respective T_g in Fig. 1. The refractive indices of the annealed films were further measured by the infrared variable angle spectroscopic ellipsometry. Fig. 3(b) shows that the evolution of the refractive index as a function of the annealing time in the films with different Ge content. Three different behaviours can be observed. With an annealing time less than 5 h, the refractive indices in Ge 17.5 and Ge20 films increase while those in Ge25 and Ge27.5 films decrease. With longer annealing time more than 5 h, the refractive indices in all the films are almost constant, which are insensitive to further prolonging annealing time. On the other hand, Ge22.5 film show negligible change in the refractive index with any annealing time, demonstrating that Ge22.5 film is the most stable against thermal annealing.

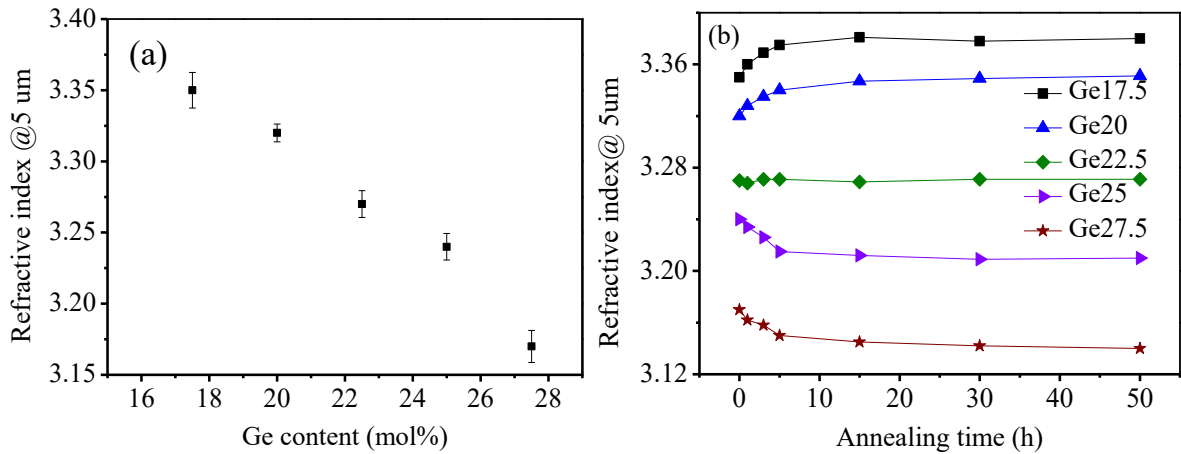


Fig. 3. (a) Ge content dependence of refractive index in GeSeTe films at the wavelength of 5000 nm. (b) annealing time dependence of the refractive index in GeSeTe films (colour online)

The optical band gap of the film was determined from the Tauc plots of the transmission spectra obtained from the films deposited on doubled polished silica wafers. The change in the bandgap as a function of Ge content is shown in Fig. 4 (a), where the bandgap increases with increasing

Ge content. This is attributed to decreasing number of lone electron pair, resulting in a decrease in the molecular orbital at the top of the valence band and an increase in the band gap [18].

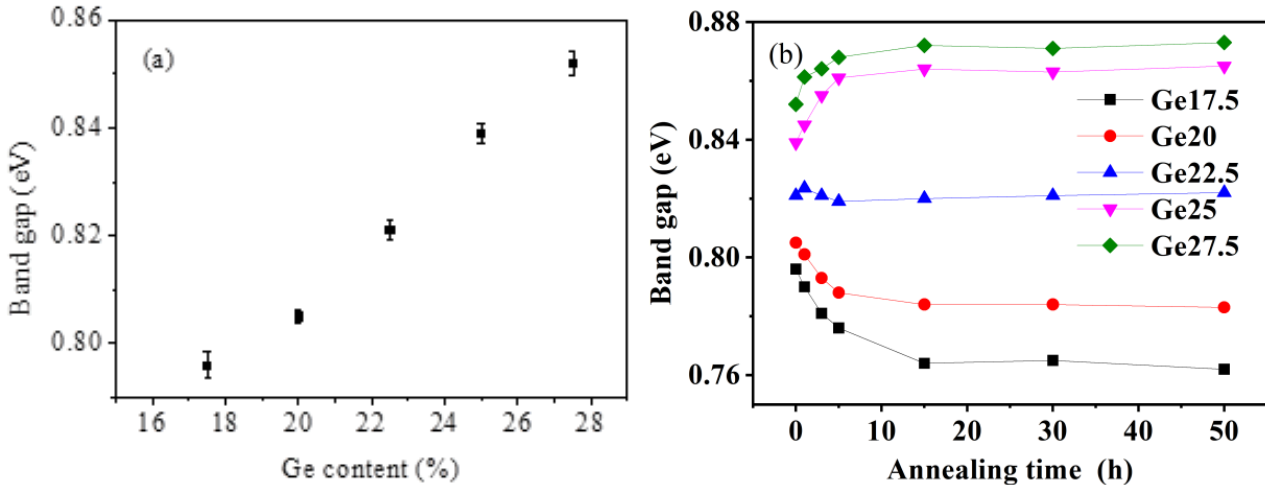


Fig. 4. (a) The dependence of the optical band gap on the Ge content in as-prepared $\text{Ge}_x\text{Se}_{10}\text{Te}_{90-x}$ films, (b) Annealing time dependent optical band gap in $\text{Ge}_x\text{Se}_{10}\text{Te}_{90-x}$ films (colour online)

Fig. 4(b) shows the optical band gap E_g for the films with different Ge contents under different annealing time. It can be found that, with increasing annealing time, E_g decreases for the films with Ge content less than 20%, while it increases for the films with Ge content more than 25 %. However, after 10 hours of annealing, E_g remains almost constant in any cases, with the exception of the film with Ge content of 22.5%, which shows negligible change in E_g over time. It is well known that, amorphous materials contain numerous defects and a high degree of disorder, which can affect the density of the localized state. While thermal annealing can trigger the conversion of the homopolar to heteropolar bonds or vice versa [19,20], this

would lead to the change of the localized state and thus the optical bandgap. A negligible change of the bandgap in the Ge22.5 film indicates that the Ge22.5 films has minimum number of defective bonds in the films investigated in the paper. This is in agreement with the mean field theory developed by J.C Philips and Thrope for chalcogenide glasses [21,22], where Ge22.5 films has a mean coordinated number of 2.45 corresponding to one of the local extremes where the stress and freedom of the atoms have a close balance, leading to a relatively stable structure against thermal annealing.

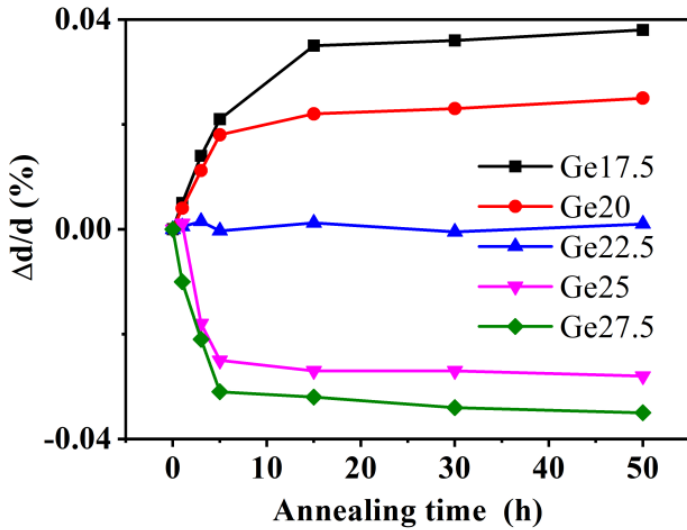


Fig. 5. Annealing time dependence of thickness change ratio ($\Delta d/d$) of $Ge_xSe_{10}Te_{90-x}$ films (colour online)

Thermal annealing also causes the change of the film thickness. We defined the film thickness ratio as:

$$\Delta d/d = (d_1 - d_0)/d_1 \quad (1)$$

where d_1 and d_0 is the thickness of initial film and annealed films, respectively. Fig. 5 shows the change of the film thickness ratio as a function of annealing time. Once again, the films with Ge content of 22.5% exhibit minimal change of the thickness ratio, while the thickness ratio of the films with Ge content of more or less than 22.5% decrease or increase with prolonging annealing time. As mentioned above, thermal annealing can trigger the bond switching from the homopolar to heteropolar bonds or vice versa. When considerable amount of the defective bonds exists in the materials, the bonding switching upon thermal annealing would cause a change of the material volume, and thus a change of the film thickness.

While chalcogenide-based optical devices are playing an important role in infrared optics, the materials with high optical and thermal stability are essential since structural relaxation caused by external energy input, like irradiation and thermal annealing, could deteriorate the performance of the optical devices. This especially happens for the planar waveguide devices where the materials should be used in the formation of thin film. While exposing to light irradiation or thermal accumulation, the change of the optical parameters in the films can seriously decrease the devices performance. Therefore, screening the optically and thermally stable film compositions has been a subject of research in the development of the high-quality optical devices based on chalcogenide glasses. The present results provide clear evidence that the $Ge_{22.5}Se_{10}Te_{67.5}$ film exhibits the smallest changes in optical band gap, refractive index, as well as thickness upon thermal annealing, and thus is expected to play an important role in planar waveguide devices.

4. Conclusion

$Ge_xSe_{10}Te_{90-x}$ ($x=17.5, 20, 22.5, 25, 27.5$) films were prepared using e-beam evaporation, and the effect of thermal annealing on their optical properties of the films was studied. With prolonged annealing time, all optical bandgap E_g , refractive index at 5000 nm, and Δd show minimal change in the films with Ge content of approximately 22.5 %. This demonstrates that $Ge_{22.5}Se_{10}Te_{67.5}$ is stable against thermal annealing and is thus the best composition for the fabrication of optical devices in the mid-infrared range.

Acknowledgements

This research has been supported by the National Natural Science Foundation of China under Youth Science Foundation Project (61805005, 62305262), the Key Program of the University Natural Science Research Fund of Anhui Province (KJ2021A0451), the International Research Cooperation Seed Fund of Beijing University of Technology (2021B34), and the project of talent introduction of Xi'an University of construction and technology (1960320034).

References

- [1] A. Zakery, S. R. Elliott, Optical Nonlinearities in Chalcogenide Glasses and their Applications, Springer-Verlag, Berlin, 151 (2007)
- [2] R. P. Wang, Amorphous chalcogenides, Pan Stanford Publishing, 2013.
- [3] K. Tanaka, K. Shimakawa, Amorphous Chalcogenide Semiconductors and Related Materials, Springer, New York, 2011.
- [4] Z. U. Borisova, Glassy Semiconductor, Springer, Boston, MA, 1981.

[5] Q. Li, R. P. Wang, Fu Xu, Xunsi Wang, Zhiyong Yang, Yin Gai, *Optical Materials Express* **10**, 1413 (2020).

[6] Z. Cernosek, E. Cernoskova, M. Hejdova, J. Holubova, R. Todorov, *Journal of Non-Crystalline Solids* **460**, 169 (2017).

[7] Martina Tomelleri, Francoise Hippert, Thierry Farjot, Christophe Licitra, Nicolas Vaxelaire, Jean-Baptiste Dory, Deniel Benoit, Valentina Giordano, Pierre Noé, *Physica Status Solidi - Rapid Research Letters* **15**, 2000451 (2020).

[8] Valerio Adinolfi, Mario Laudato, Ryan Clarke, Vijay K. Narasimhan, Lanxia Cheng, Karl Littau, *Journal of Vacuum Science and Technology A* **38**, 052404 (2020).

[9] Shun-Chang Liu, Yusi Yang, Zongbao Li, Ding-Jiang Xue, Jin-Song Hu, *Materials Chemistry Frontiers* **4**, 775 (2020).

[10] Dinesh Chandra Sati, Subhash Chander Katyal, Pankaj Sharma, *IEEE Transactions on Electron Devices* **63**(2), 698 (2016).

[11] M. Noda, A. Yoshida, T. Zrizumi, *AIP Conference Proceedings* **31**, 189 (1976).

[12] D. A. P. Bulla, R. P. Wang, A. Prasad, A. V. Rode, S. J. Madden, B. Luther-Davies, *Applied Physics A* **96**, 615 (2009).

[13] Xueqiong Su, Rongping Wang, Barry Luther-Davies, Li Wang, *Applied Physics A* **113**, 575 (2013).

[14] R. P. Wang, A. V. Rode, S. J. Madden, C. J. Zha, R. A. Javis, B. Luther-Davies, *Journal of Non-Crystalline Solids* **353**, 950 (2007).

[15] P. Sharma, S. C. Katyal, *Thin Solid Films* **517**, 3813 (2009).

[16] Thomas G. Mayerhofer, Jurgen Popp, *ChemPhysChem* **21**, 1218 (2020).

[17] P. Knotek, P. Kutalek, E. Cernoskova, M. Vlcek, L. Tichy, *RSC Advances* **10**, 42744 (2020).

[18] M. Kastner, *Physical Review Letters* **28**, 355 (1972).

[19] Yuanhuan Sun, Zheng Zhang, Zhen Yang, Lei Niu, Jian Wu, Tengxiu Wei, Kunlun Yan, Yan Sheng, Xunsi Wang, Rongping Wang, *Optical Materials Express* **11**(8), 2413 (2021).

[20] Jingshuang Qin, Jinbo Chen, Yimin Chen, Jierong Gu, Xiang Shen, Rongping Wang, *Optical Materials Express* **10**(11), 2944 (2020).

[21] J. C. Phillips, *Journal of Non-Crystalline Solids* **34**, 153 (1979).

[22] M. F. Thrope, *Journal of Non-Crystalline Solids* **57**, 355 (1983).

Corresponding author: nysxq@bjut.edu.cn